International Journal of Chemical, Materials and Biomolecular Sciences
ISSN: 2415-6620
Vol:7, No:12, 2013

Dripping Modes of Newtonian Liquids: The Effect of Nozzle Inclination

Amaraja Taur, Pankaj Doshi, Hak Koon Yeoh

***Abstract*—**The dripping modes for a Newtonian liquid of viscosity μ emanating from an inclined nozzle at flow rate Q is investigated experimentally. As the liquid flow rate Q increases, starting with period-1 with satellite drops, the system transitions to period-1 dripping without satellite, then to limit cycle before showing chaotic responses. Phase diagrams showing the changes in the transitions between the different dripping modes for different nozzle inclination angle θ is constructed in the dimensionless (Q, μ) space.

***Keywords*—** Dripping, inclined nozzle, phase diagram.

I. INTRODUCTION

THE drop formation resulting from the breakup of an axisymmetric liquid jet injected from a vertical nozzle has been an interesting area, as it has many industrial applications such as ink-jet printing [1], silicon microstructure [2], microencapsulation [3], 3D printing [4]. The phenomenon of drop formation from a vertical nozzle has been broadly studied from many decades. Eggers [5] provided an extensive review about the experimental and computational work on this study starting from 1686.

In the process of drop formation, dripping mode is characterized by tiny droplets emanating from the nozzle at low flow rate [6]-[9], while jetting mode occurs at high flow rates in which liquid flows out as a continuous stream to form a jet which subsequently breaks up in to small droplets [10], [11]. In dripping mode, before the drop breaks from the remaining part of the fluid, the gravitational and surface tension forces are balanced. If inertia does not play any role then liquid drop goes through sequence of equilibrium shapes [12].

A Newtonian liquid having viscosity μ, density ρ, and surface tension σ, flowing through a nozzle of outer radius R, at flow rate Q is the most commonly investigated configuration. For a vertical nozzle the dripping dynamics are governed by three dimensionless groups [13]-[15]: Weber number $We\equiv \rho v^2R/\sigma$ that measures the relative importance of inertia to surface tension force, Bond number $G\equiv \rho gR^2/\sigma$, where g is the acceleration due to gravity, that measures the relative importance of body force to surface tension force, and Kapitza number $Ka\equiv (\mu^4 g/\rho\sigma^3)^{1/3}$ or Ohnesorge number $Oh=\mu/(\rho R\sigma)^{1/2}$, both measure the relative importance of viscous force to surface tension force.

The viscosity effects on drop shapes and liquid thread length have been studied by using high speed photography [16]. This work is later extended and to examine the effect of all relevant parameters likes flow rate, viscosity, nozzle diameter, and nozzle thickness on the general characteristics of drop formation especially the growth, extension, breakup of liquid thread, and satellite drop formation that are formed following the pinch off process [8]. Several studies on drop formation by changing liquid flow rate showed a pronounced effect on dripping dynamics where at low flow rate simple dripping is observed followed by the complex dripping at moderate flow rate, and at high flow rate system gives jets of the liquid [8], [14], [17]. A detailed phase diagram showing these transitions from simple and complex dripping and jetting in (*We*, *Oh*) space are developed and critical *We* for these transitions are estimated by scaling argument and shown to accord well with simulations [13].

The introduction of asymmetrical perturbations, both by tilting the nozzle by an angle θ from the vertical [18], or by cutting obliquely the tip of nozzle [19], breaks the cylindrical symmetry and found strong changes in the dripping dynamics when compared with those obtained with flat tip shaped nozzle in the vertical position. In the rare experiments of dripping from a tilted nozzle, it is showed that the θ can constitute an effective control parameter by breaking the axis symmetry [18] thus adding asymmetric perturbations [19] as well as changing the effective *G*. However, previous studies are far from being comprehensive, thus unable to provide guides on the general behavior. The goal of this paper is to further explore the effects of θ and the associated parameters to avail a more complete picture for future theoretical analysis.

The paper is organized as follows: Section II describes the experimental setup, material properties, and experimental procedure. Section III presents and discusses the experimental results before concluding in Section IV.

Amaraja Taur is with the Department of Chemical Engineering, Faculty of Engineering, University of Malaya, 50603, Kuala Lumpur, Malaysia (e-mail: amarajataur@gmail.com).

Dr. Pankaj Doshi is with the Chemical Engineering and Process Development division, National Chemical Laboratory, 411008, Pune, India (e-mail: p.doshi@ncl.res.in).

Dr. Yeoh Hak Koon is with the Department of Chemical Engineering, Faculty of Engineering, University of Malaya, 50603, Kuala Lumpur, Malaysia (e-mail: yeohakoon@um.edu.my).

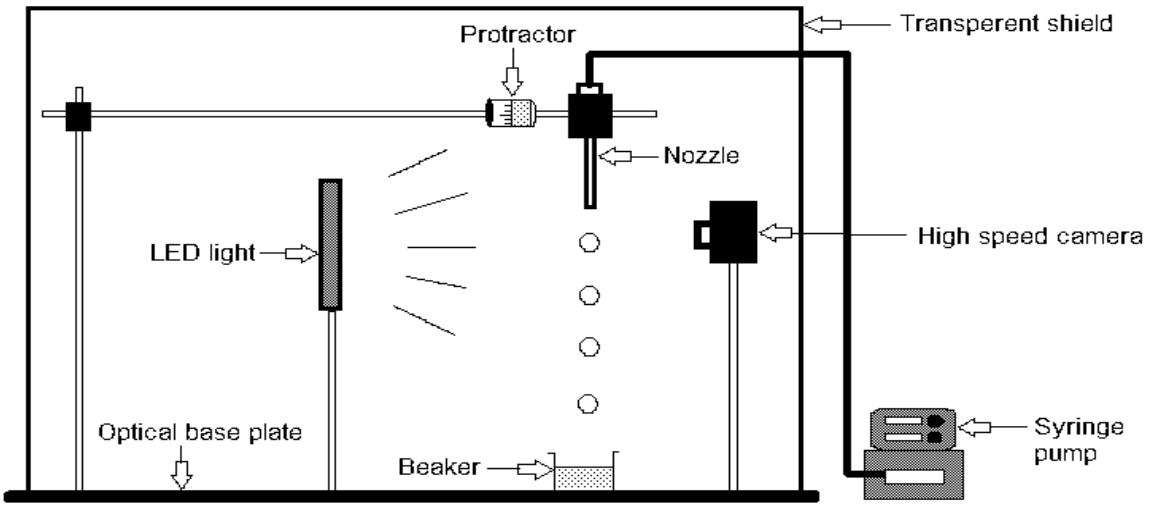

Fig. 1 Schematics of the experimental setup

II. Methods

A. Apparatus

The experimental apparatus is depicted in Fig. 1. It consists of a nozzle through which liquid flows to form drops. The liquid is delivered to the nozzle by using a Meditech JZB-1800D Syringe Pump which is capable of providing range of flow rate from 0.00167 to 30 mL/min with an accuracy of ±2%. Two stainless steel dispensing nozzles (P-30619-06 and P-30619-07) are obtained from Cole-Parmer. The outer diameters of the nozzles are 1/32" (N1) and 1/8" (N2). The ratio of the inner radius to outer radius is >0.2, hence the effect of nozzle thickness on the interface dynamics can be safely neglected [8]. A protractor is provided to adjust the tilt angle of the nozzle. A transparent shield is provided to reduce draft that can perturb the drop formation process.

The high speed camera is Casio EX-FH100 capable of recording 30 to 1000 frames per second. A planar white LED backlight measuring 10cm × 10cm (model LFL-Si100-W-IP65) with adjustable brightness is obtained from Falcon Illumination (M) Pte. Ltd.

The sharpness of the images can be adjusted via the intensity of the backlight, the focal length and digital zoom of the camera. All parts of apparatus except the syringe pump are kept on a 0.3m×0.3m×0.06m aluminum optical base plate inside the transparent shield.

B. Chemicals Used

A mixture of water and glycerol chosen as an experimental liquid because of their desirable physical properties namely, that their surface tension and densities are almost similar to that of pure water, but their viscosities can be made to vary three orders of magnitude. The 99% pure glycerol was obtained from R and M Chemicals, CAS NO [56-81-5], and used as obtained. Distilled water is used to the make water glycerol mixtures. Silicone oil, Dow Corning® 111 Valve Lubricant and Sealant was used for dewetting of the outer nozzle surface. The physical properties of these are taken from the literature [20] and are listed in Table I.

III. Results and Discussions

A. Dripping Modes

Experiments with a vertically oriented nozzle illustrate the various dripping modes observed. Fig. 2 shows the variation with drop numbers of t_b made dimensionless with the capillary time $(\rho R^3/\sigma)^{1/2}$. As depicted in Fig. 2 (a), values of t_b decrease with increase in Weber number. Based on this, three different dripping regimes were encountered, namely period-1 (P1); limit cycle (LC), and chaos (C). Unlike reports in the literature [15], for this chosen value of G, no satellite drops are observed at very low values of We. At low Weber numbers, all the droplets have values of t_b within ±10% of the average, and this is denoted as the period-1 (P1) dripping. Seen on the time return map in Fig. 2 (b), the points cluster together, ideally forming only one point. At moderate Weber numbers, the t_b trajectory repeats itself but the variation in t is more than 10% of its average value. This is denoted as the limit cycle (LC) behavior. On the time return map, the trajectory encircles a region. The chaotic (C) behavior is seen at high Weber numbers, where the t_b trajectory does not repeat itself, showing disorderly long term evolution. On the time return map, the points are scattered rather randomly.

TABLE I
PHYSICAL PROPERTIES OF WATER GLYCEROL MIXTURE

Solution	Wt. % glycerol	ρ (kg/m^3)	μ (mPa.s)	σ (mN/m)
S0	0	1000	1	72
S20	20.0	1044	1.5	69.5
S40	40.0	1095	3.2	68.4
S80	80.0	1205	45.9	64.7

The two Weber numbers for the transition from one mode to another can be pin-pointed experimentally. The first, for transition from P1 to LC occurs at $We = We_{LC}$, and the second, for transition from LC to C occurs at $We = We_c$. As the value of *Ka* changes, the corresponding values of We_{LC} and We_c also change. These transitional *We* are plotted against *Ka* as a dripping mode phase diagram next.

B. Phase Diagram for Dripping Modes

The phase diagrams shown in Figs. 3 (a)-(c) identify the location in the parameter space where the dynamics changes from one mode to another. For a vertical nozzle (Fig. 3 (a)), at low values of *Ka*, both We_{LC} and We_c rise sharply as the value of Ka increases. For high values of *Ka*, the trajectories of We_{LC} and We_c converge, i.e. the transition occurs directly from P1 to C without exhibiting a LC regime [15]. A feature of interest to applications is that the P1 region widens considerably at high values of *Ka*. Other than the absence of a satellite dripping mode, this phase diagram is qualitatively similar to that reported by Hariprasad et al. [15].

The phase diagrams for an inclined nozzle look similar to that of the vertical nozzle. On closer examination, three significant and potentially useful features can be distilled. First, the values of We_c decrease dramatically with θespecially for $Ka \sim 10^{-3}$, suggesting that the asymmetry favours chaotic dripping. This is in line with the findings of Reyes et al. [18], which showed that even at $\theta = 5^o$, the dripping dynamics turns very complicated. Second, the locus of We_{LC} is not so strongly affected by θ at low values of *Ka*. It suggests that P1 and LC regimes are influenced more by viscous damping than by asymmetry. A consequence of these two observations is that the LC regime shrinks noticeably with increase in θ. Conceivably at even larger values of θ, the LC region might vanish.

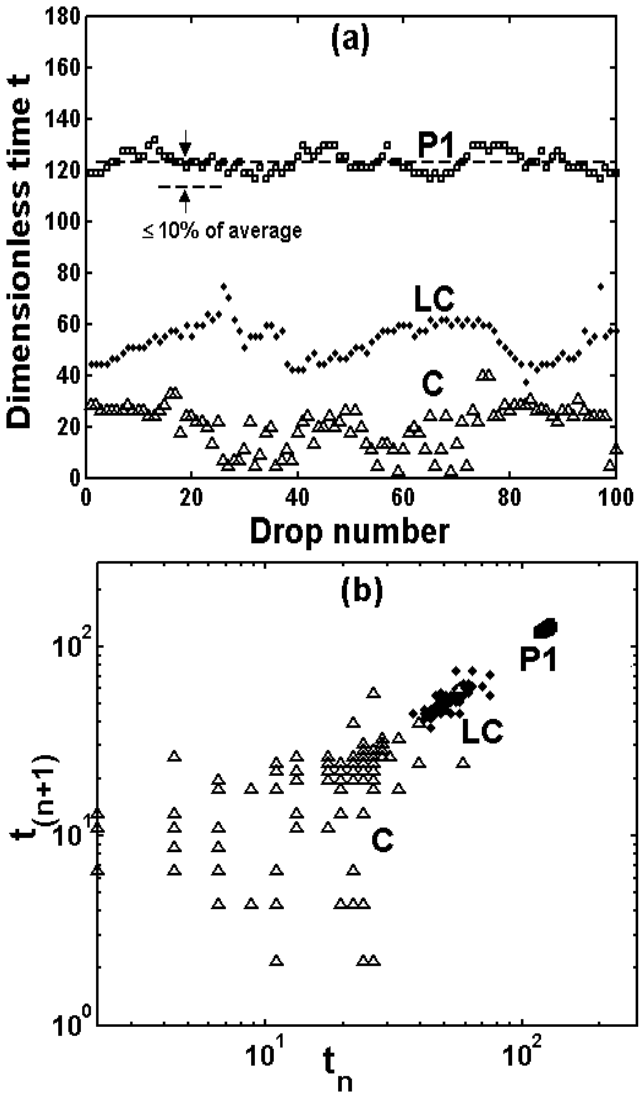

Fig. 2 (a) Variation of the dimensionless dripping time with drop number, and (b) the corresponding time return map for a vertical nozzle. Three different dripping behaviours are seen as *We* increased, namely P1 (□ We=0.05), LC (◆ We=0.15), and C (△ We=0.30). Here G=0.062, Ka=0.000562

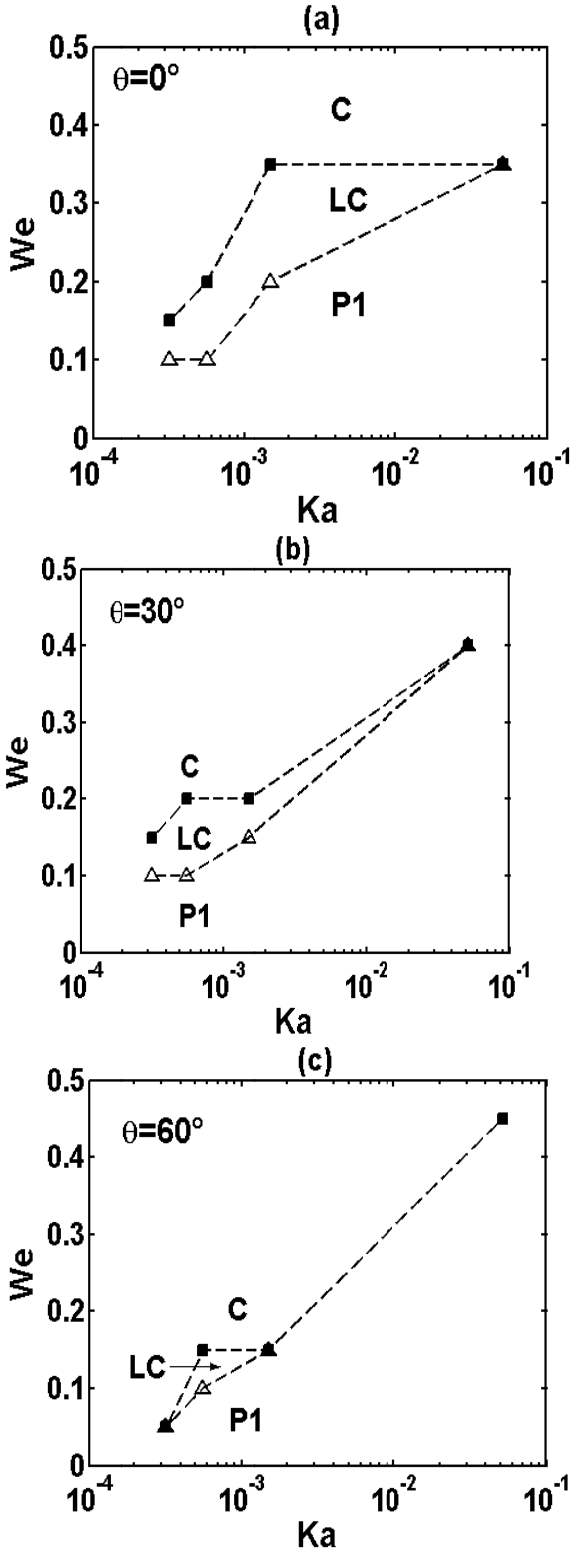

Fig. 3 An experimental phase diagram in (*We*, *Ka*) space at θ=0° (a), θ=30° (b), θ=60° (c), showing transitional Weber numbers
We_{LC} We_c, where G=0.062

At high values of *Ka*, however, the interaction of asymmetry with strong viscous damping raises the values of We_{LC}, leading to the third observation: The values of *We* for direct transition from P1 to C increase with θ. This avails an operating option to move the chaotic dripping of a very viscous liquid into the well-defined P1 region simply by tilting the nozzle. The modest increase in the values of this direction transition *We* against the corresponding values for the vertical nozzle suggest that the effect of θ is most likely a higher order effect and thus difficult to deduce from scaling arguments [15].

C. Satellite Drop Formation

In our experiments, satellite drop formation was observed only with the larger nozzle with nearly ten times higher Bond number (*G*=0.61). This is in accord with reports that larger values of G give rise to richer dripping dynamics [15]. The dripping mode remains at P1 (t_b is based on the primary drop), only that each primary drop is followed by another tiny satellite drop. Following Hariprasad et al. [15], this region is labeled as P1S. Fig. 4 shows the transition from P1S to P1 in the (*We, Ka*) space, with the corresponding transition *We* labeled as We_{P1}. Note that Fig. 4 is an incomplete phase diagram that highlights only the P1S-P1 region. Clearly We_{P1} is not strongly affected by *Ka*, in agreement with literature [15].

Interestingly, by changing the values of θ, the values of We_{P1} also do not change appreciably. This counter-intuitive observation is not surprising as it has been shown via detailed computational studies [21] that satellite formation is the consequence of a localized high speed drainage effect. The downside of this is that unwanted satellites will not disappear by merely tilting the nozzle.

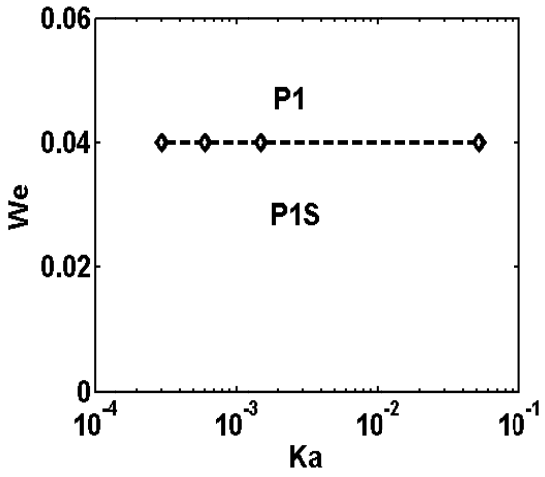

Fig. 4 Phase diagram in (*We*, *Ka*) space focusing on the transition from P1S to P1 dripping when *G*=0.61. The transition line at θ=0°, θ=30°, and θ=60° are indistinguishable

IV. Conclusion

This is the first systematic exploration of the phase diagram for dripping at non-zero θ. According to the foregoing results, the global dripping behavior from an inclined nozzle is similar to that from a vertical nozzle, but modified where an increase in θ results in a narrowing of the LC regime and giving an extended P1 regime. Further, as expected, satellite formation is unaffected by θ. These findings have implications to applications involving droplet formation, as they clarify another heretofore under-studied parameter to tune the dripping mode. The study on the effect of θ on drop volumes is underway. Future directions may include computational studies to elucidate the detailed changes in flow profiles that lead to the macroscopic observations.

Acknowledgment

This work was supported by FRGS grant FP059-2010B and PPP grant PG091-2012B. The authors thank University of Malaya for sponsoring a trip of Dr. Pankaj Doshi to Malaysia.

References

[1] H. P. Le, "Progress and trends in ink-jet printing technology," Journal of Imaging Science and Technology 42, 49-62 (1998).
[2] T. Laurell, J. Nilsson and G. Marko-Varga, "Silicon microstructures for high-speed and high-sensitivity protein identifications," Journal of Chromatography B: Biomedical Sciences and Applications 752, 217-232 (2001).
[3] S. Freitas, H. P. Merkle and B. Gander, "Microencapsulation by solvent extraction/evaporation: reviewing the state of the art of microsphere preparation process technology," Journal of Controlled Release 102, 313-332 (2005).
[4] E. M. Sachs, J. S. Haggerty, M. J. Cima and P. A. Williams, "Three dimentional printing techniques", (US Patent 5,340,656, 1994).
[5] J. Eggers, "Nonlinear dynamics and breakup of free-surface flows," Reviews of modern physics 69, 865 (1997).
[6] J. Eggers, "Theory of drop formation," Physics of Fluids 7, 941-953 (1995).
[7] R. Schulkes, "The evolution and bifurcation of a pendant drop," Journal of Fluid Mechanics 278, 83-100 (1994).
[8] X. Zhang and O. A. Basaran, "An experimental study of dynamics of drop formation," Physics of fluids 7, 1184 (1995).
[9] X. Zhang, "Dynamics of growth and breakup of viscous pendant drops into air," Journal of colloid and interface science 212, 107-122 (1999).
[10] L. Rayleigh, "On the capillary phenomena of jets," Proceedings of the Royal Society of London 29, 71-97 (1879).
[11] L. Rayleigh and J. W. Strutt, "On the instability of jets," Proceedings of the Royal Mathematical Society London 4-13 (1879).
[12] A. M. Worthington, "On pendent drops," Proceedings of the Royal Society of London 32, 362-377 (1881).
[13] B. Ambravaneswaran, H. J. Subramani, S. D. Phillips and O. A. Basaran," Dripping-jetting transitions in a dripping faucet," Physical review letters 93, 034501 (2004).
[14] B. Ambravaneswaran, S. D. Phillips and O. A. Basaran, "Theoretical analysis of a dripping faucet," Physical review letters 85, 5332 (2000).
[15] H. J. Subramani, H. K. Yeoh, R. Suryo, Q. Xu, B. Ambravaneswaran and O. A. Basaran, "Simplicity and complexity in a dripping faucet," Physics of fluids 18, 032106 (2006).
[16] X. Shi, M. P. Brenner and S. R. Nagel, "A cascade of structure in a drop falling from a faucet," Science-New York then Washington 219-219 (1994).
[17] C. Clanet and J. C. Lasheras, "Transition from dripping to jetting," Journal of Fluid Mechanics 383, 307-326 (1999).
[18] M. Reyes, R. Pinto, A. Tufaile and J. Sartorelli, "Heteroclinic behavior in a dripping faucet experiment," Physics Letters A 300, 192-198 (2002).
[19] A. D'Innocenzo, F. Paladini and L. Renna, "Experimental study of dripping dynamics," Physical Review E 65, 056208 (2002).
[20] www.aciscience.org,"Physical properties of glycerine and its solutions", (1967).
[21] E. D. Wilkes, S. D. Phillips and O. A. Basaran, "Computational and experimental analysis of dynamics of drop formation," Physics of fluids 11, 3577 (1999).